THE JOURNAL OF PHYSICAL CHEMISTRY B

ARTICLE

pubs.acs.org/JPCB

Solvent-Induced Protein Refolding at Low Temperatures

Yasar Akdogan and Dariush Hinderberger*

Max Planck Institute for Polymer Research, Ackermannweg 10, 55128 Mainz, Germany

Supporting Information

ABSTRACT: Protein refolding at low temperatures is shown for a self-assembled system of human serum albumin (HSA) and spin-labeled fatty acids (FAs), in ternary solvent mixtures with usually denaturing cosolvents ethanol or ionic liquids (ILs). When HSA is natively folded, it offers FA binding sites, and the uptake and the distribution of these FA binding pockets have characteristic continuous wave electron paramagnetic resonance (CW EPR) and double electron−electron resonance (DEER) signatures. At room temperature, CW EPR shows that the addition of 35% (v/v) of ethanol or IL leads to HSA being unfolded. A temperature decrease yields bimodal CW EPR spectra with bound FA and free FA signals, indicating at least partial refolding of HSA, which is also confirmed by corresponding DEER data. This finding is based on increased protein stability at lower temperatures and a change in the preferential solvation of the protein by glycerol in the ternary solvent mixtures.

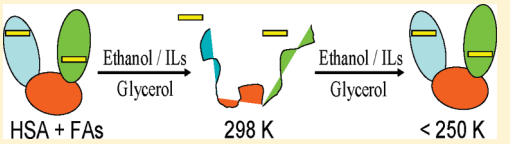

INTRODUCTION

Protein denaturation involves any major change of the native protein structure leading to loss of activity usually caused by organic solvents, inorganic salts, extreme pH values, external stress, or low and high temperatures.[1] Many studies have been performed concerning the denaturing of the structure of serum albumin owing to its role as a model protein.[2] In particular, human serum albumin (HSA) is the most abundant protein in human blood plasma and serves as a carrier of fatty acids (FAs) and a diverse range of metabolites from the bloodstream to target cells. It consists of a 585 amino acid residue monomer and three homologous α-helical domains (I−III) with a molar mass of ca. 66 kDa (Figure 1 (A)).

The denaturation of proteins upon heating is a well-known phenomenon. On the contrary, cold denaturation that occurs on cooling the protein below room temperature (RT) is less known.[3−5] Increasing the temperature leads to heat absorption that is followed by an increase in overall enthalpy and entropy. Therefore, the denaturation of a protein at high temperatures is an expected effect. For example, thermal changes of HSA in solution indicate that a temperature rise from RT to 328 K results in a reversible unfolding of the protein. However, increasing the temperature to 343 K induces irreversible conformational changes in the structure of HSA.[6] Furthermore, in the presence of a denaturating agent such as ethanol, the thermal stability of HSA decreases.[7] On the other hand, low-temperature destabilization of proteins is explained by the specific and temperature-dependent interactions between the protein's nonpolar groups and water, which favor disordered or unfolded conformations of the protein.[8] Pastore et al. characterized both the cold and hot thermal denaturation (unfolding) of yeast frataxin, Yfh 1, at 280 and 304 K, respectively, by using NMR and CD methods.[5] The cold denaturation state cannot be detected for all proteins since cold denaturation of most proteins occurs below the freezing point of water. Therefore, it is necessary to raise the temperature of cold denaturation using chemical denaturants, extreme pH values, or high pressures.[9,10]

Alternatively, the freezing point of water can be dropped by addition of cryoprotectants. Ice formation in protein solutions may cause irreversible protein denaturation and loss of protein activity. Glycerol is a trialcohol and is used as the standard cryoprotectant to protect proteins against water freezing in many experimental techniques.[11,12] Furthermore, glycerol stabilizes the folded structure of proteins in solution. Rariy et al. showed that unfolded and reduced hen egg-white lysozyme was refolded and reoxidized in 20% (v/v) glycerol-containing water solutions with a yield of 61%, and in contrast the refolding yield was only 38% in pure water.[13]

This work focuses on the effects of low and high temperatures in combination with denaturating cosolvents on the functional solution structure of HSA. Of these cosolvents, 15% (v/v) of glycerol, a well-known nondenaturating cosolvent, is used for all solutions to avoid ice formation, achieve vitrification, and reach lower glass transition temperatures. Ethanol, on the other hand, is a well-known denaturating solvent for HSA. Additionally, imidazolium-based ionic liquids (ILs) denature the native structure of HSA.[14−16] The unique properties of ILs, including high thermal and chemical stability, negligible vapor pressure, low degree of flammability, and low toxicity, have made them alternative solvents to traditional organic solvents. Their physical properties such as polarity, viscosity, miscibility, and density can be finely tuned to fulfill specific demands by the selection of suitable anions and cations.[17−19] The denaturating effects of six different ILs based on 1-ethyl-3-methyl imidazolium (Emim) as a

Received: October 7, 2011
Revised: November 23, 2011
Published: November 24, 2011

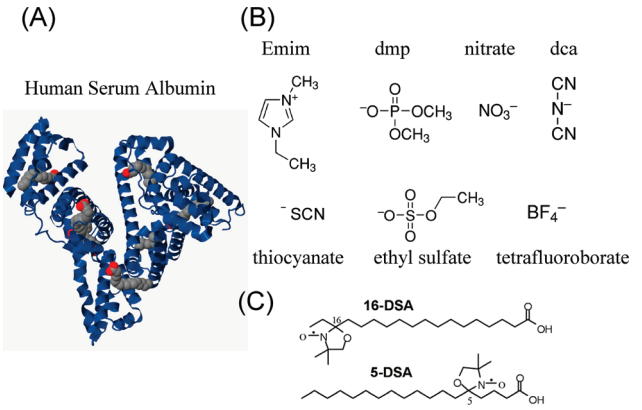

Figure 1. (A) Crystal structure (PDB 1e7i) of HSA cocrystallized with seven fatty acid molecules (ref 23). The oxygen atoms of the FA carboxylic acid headgroups are displayed in red. (B) Chemical structures of the cation (Emim) and anions (dimethyl phosphate, dmp; nitrate; dicyanamide, dca; thiocyanate; ethyl sulfate; and tetrafluoroborate) used as imidazolium-based ionic liquids. (C) Chemical structures of the EPR-active FAs, 16-doxylstearic acid (16-DSA) and 5-doxylstearic acid (5-DSA).

cation with different anions, dimethyl phosphate (dmp^-), nitrate (NO_3^-), tetrafluoroborate (BF_4^-), ethyl sulfate ($EtSO_4^-$), thiocyanate (^-SCN), and dicyanamide (dca^-), are compared with the denaturating effect of ethanol (Figure 1(B)).

Recently, we have shown that addition of imidazolium-based ILs to an aqueous solution of HSA/fatty acid conjugates was accompanied by significant destabilization and unfolding of the protein's tertiary structure.[16] In contrast, HSA maintains its tertiary structure when the IL choline dihydrogenphosphate (dhp) was added. However, the HSA solutions in this prior study were binary mixtures of aqueous buffer/IL and did not contain glycerol, so these results use the added ILs as cryoprotectant. In the current study, we now use glycerol in addition, which lowers the glass transition temperature of the complete system to illustrate the solvent effects that even lower temperatures have on the protein structure.

Electron paramagnetic resonance (EPR) spectroscopy in combination with site-directed spin labeling has been increasingly used to reveal the molecular and global structure of proteins and their local dynamics.[20−22] Here, the spin-labeled fatty acids, 5- and 16-doxylstearic acid (DSA), are mixed with HSA to obtain information on the HSA structure (Figure 1(C)). Our approach hence is one type of *site-directed spin probing*, in which the EPR active molecules are noncovalently attached to (in this case) the protein of interest.

Crystallographic analysis revealed seven distinct binding sites for long-chain FAs.[23] These binding sites are composed of positively charged amino acids as anchoring units, which electrostatically interact with the carboxylic acid headgroup of FA, and long, hydrophobic pockets surrounding the methylene tail.[24] Therefore, our spin probe 5-DSA, which has the EPR-active nitroxide moiety close to the carboxylic acid, probes the ionic anchor points inside the binding channels, while 16-DSA, which is labeled at the far end of the alkyl chain, probes the entry points into the FA channels.[25] Conventional continuous wave (CW) EPR spectroscopy clearly allows discerning whether FAs are bound to HSA or not through their sensitivity to the rotational dynamics of the spin probes. Pulse EPR techniques, such as double electron−electron resonance (DEER) spectroscopy under the experimental conditions here, can access distances up to 6 nm between the spin-labeled FAs bound to HSA. Thus, the FA distribution obtained by DEER spectroscopy provides an indirect yet effective way to characterize the structure of the protein, which is an alternative technique to NMR and X-ray crystallography.[16,25−27]

Here, we specifically aim at studying the solution structure and dynamics of HSA with and without denaturating cosolvents in particular at low temperatures. These temperatures span from 323 K down to the glass transition temperature of the water/glycerol(-denaturant)-based solutions. First, we present the results that adding low concentrations of denaturants 5% (v/v) to HSA solutions has on the detectable functional structure of HSA. We then show how HSA is unfolded at RT upon addition of 35% (v/v) of ethanol or ILs and discuss how its structural changes depend on the temperature. For this, we exploit the fact that denaturation of HSA in solution upon addition of cosolvents (ethanol or ILs) can easily be detected through CW EPR spectroscopy by analyzing the ratio of bound/free FAs at different temperatures. However, different from what is known of cold denaturation of proteins in the literature, our combined results of CW EPR spectroscopy at various temperatures and DEER spectroscopy at 50 K illustrate that denatured HSA upon addition of certain cosolvents even refolds when lower temperatures can be achieved before freezing, which in our case is made possible by adding glycerol to all samples.

EXPERIMENTAL PROCEDURES

Materials. Nondenatured HSA (>95%, Calbiochem), spin-labeled FAs 5- and 16-DSA ethanol, the ILs 1-ethyl-3-methylimidazolium dimethylphosphate (Emimdmp, >98.5%), Emim tetrafluoroborate ($EmimBF_4$, >99%, Sigma-Aldrich), Emim nitrate ($EmimNO_3$, >99%), Emim ethyl sulfate ($EmimEtSO_4$, >98.5%), Emim thiocyanate (EmimSCN, >99%), and Emim dicyanamide (Emimdca, >%98.5), and 87 wt % glycerol (13 wt % water) were used as received from Sigma-Aldrich.

Sample Preparation. Aqueous solutions of 2 mM HSA in 0.11 M phosphate buffer (pH 7.2) and 26 mM DSA in 0.1 M KOH were prepared. The concentration of DSA in the final buffered solutions of pH 7.4 was kept constant at 1.5 mM. The molar ratio of DSA per protein molecule was kept constant at 2:1. Different amounts of ionic liquids and ethanol (5, 35, 42% (v/v)) were added to these aqueous FA/HSA solutions. $EmimBF_4$, $EmimEtSO_4$, EmimSCN, and Emimdca are liquid at RT. Emimdmp and $EmimNO_3$ were first heated to a liquid phase. All ILs are water-miscible. Glycerol (15% (v/v)) was added to all the aqueous solutions. No changes in the CW EPR spectra at RT were observed upon addition of glycerol. About 100 μL of the final solutions was filled into 3 mm (outer diameter) quartz tubes and shock-frozen in liquid nitrogen cooled iso-pentane.

EPR Measurements. A Miniscope MS200 (Magnettech, Berlin, Germany) benchtop spectrometer was used for X-band continuous wave (CW) EPR measurements at a microwave frequency of ~9.4 GHz. The spectrometer is equipped with a temperature control unit TC H02 (Magnettech), providing for an electronic adjustment in steps of 0.1 K in the possible range of 103−473 K. Measurements were performed for the temperature range between 103 and 323 K using a modulation amplitude of 0.05 mT. The microwave frequency was recorded with a frequency counter, model 2101 (Racal-Dana).

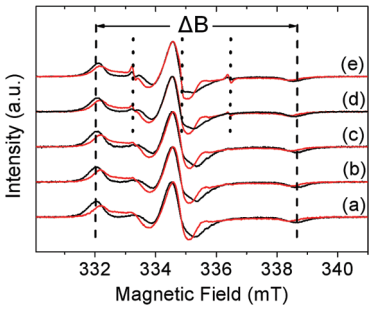

Figure 2. CW EPR spectra of 5-DSA (black) and 16-DSA (red) in HSA buffer/15% (v/v) glycerol (a) at a FA/HSA ratio of 2 upon addition of 5% (v/v) ethanol (b), Emimdmp (c), $EmimBF_4$ (d), or Emimdca (e) at 298 K. The characteristic features for slow rotational motion and fast rotational motion are marked by dashed lines and dotted lines, respectively. The spectral separation of the outer extrema ΔB is indicative of slow rotational motion and is indicated by a two-headed arrow.

The four-pulse DEER sequence $\pi/2(\nu_{obs}) - \tau_1 - \pi(\nu_{obs}) - (\tau_1 + t)(\nu_{pump}) - (\tau_2 - t) - \pi(\nu_{obs}) - \tau_2 -$ echo was used to obtain dipolar time evolution data at X-band frequencies (9.2−9.4 GHz). DEER experiments were performed on a Bruker Elexsys 580 spectrometer equipped with a Bruker Flexline split-ring resonator ER4118X_MS3.[28,29] The dipolar evolution time t was varied, whereas $\tau_2 = 2.5\ \mu s$ and τ_1 were kept constant. Proton modulation was averaged by the addition of eight time traces of variable τ_1, starting with $\tau_{1,0} = 200$ ns and incrementing by $\Delta\tau_1 = 8$ ns.[30] The resonator was overcoupled to $Q \approx 100$. The pump frequency, ν_{pump}, was set to the maximum of the EPR spectrum. The observer frequency, ν_{obs}, was set to ν_{pump} + 61.6 MHz, coinciding with the low-field local maximum of the nitroxide spectrum. The observer pulse lengths were 32 ns for both $\pi/2$ and π pulses, and the pump pulse length was 12 ns. The temperature was set to 50 K by cooling with a closed cycle cryostat (ARS AF204, customized for pulse EPR, ARS, Macungie, PA). The raw time domain DEER data were processed with the program package DeerAnalysis2008.[31] Intermolecular contributions were removed by division by an exponential decay with a fractal dimension of $d = 3.8$. As shown in a previous study, the deviation from $d = 3.0$ (which would be expected for a homogeneous three-dimensional background distribution) originates from excluded volume effects due to the size of the protein.[25] However, for samples which contain 35% or 42% (v/v) of cosolvents, a background dimensionality of $d = 3.0$ could be used again, as the protein structure is severely altered and (see below) loss of tertiary structure is reflected in the loss of excluded volumes, which finally leads to the reduced background dimensionality as compared to the natively folded protein. The resulting time traces were normalized to $t = 0$. The number of average dipolar coupled spins, N, was calculated by the relation[32]

$$N = \frac{\ln(1-\Delta)}{1-\lambda} + 1 \qquad (1)$$

where Δ is the modulation depth $\Delta = 1 - \lim_{t\to\infty} V(t)/V(0)$, and λ is the inversion efficiency of the pump pulse. In this study, the inversion efficiencies of $\lambda = 1.29$ (5-DSA) and $\lambda = 1.37$ (16-DSA) were determined using the 2:1 (FA:HSA) buffered sample as references.[26] Distance distributions were obtained by Tikhonov regularization using regularization parameters of 100 and 1000 for 16-DSA and 5-DSA, respectively.

RESULTS AND DISCUSSION

Effects of Low and High Concentrations of Cosolvents on HSA Solution Structure. *Addition of 5% (v/v) of Denaturing Solvents: CW EPR Results.* In a typical CW EPR spectrum of spin-labeled FAs at 298 K, bound FAs (immobilized) have characteristic broad outer hyperfine features stemming from restricted rotational motion, and free FAs (mobilized) can be recognized through sharp three-line signals, signatures of freely tumbling DSA. Figure 2 shows the CW EPR spectra of the spin-labeled FAs, 5-DSA and 16-DSA, in different HSA solutions upon addition of 5% (v/v) of ethanol or ILs. The FA/HSA ratio is kept constant at 2:1.

In the HSA buffer/glycerol solutions, the separation of the outer extrema in the spectra, ΔB, is remarkably different for 5-DSA and for 16-DSA (Figure 2(a)). Although these CW EPR spectra were simulated and the rotational motion was quantified, e.g., by the rotational correlation time τ_c (see Supporting Information Figure 1 and Table 1), it is much simpler and yet similarly illuminating to analyze the spectral separation ΔB. ΔB is also very sensitive to the rotational motion of slowly tumbling spin labels, with a larger value in general corresponding to a more restricted motion. The larger ΔB value and more restricted motion of 5-DSA compared to that of 16-DSA agrees well with the description that 5-DSA probes the inside the FA binding channels close to the anchor points, while 16-DSA probes the entry points of the channels, where it has more rotational freedom. However, the ΔB values of 5-DSA decrease upon addition of 5% (v/v) of imidazolium-based ILs or ethanol, indicating a measurable effect on the tertiary structure of HSA. Especially, in 5% (v/v) added Emimdca (Figure 2(e)), the ΔB value of 5-DSA decreases, and it gets closer to the ΔB of 16-DSA. This suggests that the FA binding channels may widen, so that the rotational motion of 5-DSA is less restricted. On the other hand, the ΔB values of 16-DSA remain very similar in Figure 2-(a−e), probably since 16-DSA motion is less restricted even before IL or ethanol addition such that a potential additional effect is not observable.

Moreover, the addition of 5% (v/v) of Emimdca (Figure 2(e)) results in a stronger spectral contribution of free FAs (typical three-line CW EPR spectrum, indicated by the dotted lines in Figure 2), as compared with those found with other ILs or ethanol. This could be explained, e.g., by assuming that even at a low volume fraction Emimdca either competitively occupies the FA binding sites or partially denatures HSA, or both. In contrast, ΔB does not change after addition of 5% (v/v) of ethanol or Emimdmp. Also, other ILs with the same Emim cation and with different anionic groups such as nitrate (NO_3^-), ethyl sulfate ($EtSO_4^-$), and thiocyanate (^-SCN) are used to observe the effect of specific IL-based anions on albumin structure. Figure 2 in the Supporting Information displays the CW EPR spectra of 5-DSA in different HSA solutions upon addition of all used 5% (v/v) ILs and ethanol at RT. The amount of free FAs and the decrease of ΔB compared to those in HSA buffer/glycerol solutions become larger in the following order: addition of ethanol ∼ Emimdmp < $EmimNO_3$ ∼ $EmimBF_4$ < $EmimSO_4$ ∼ EmimSCN < Emimdca. Emimdca clearly has the strongest effect.

Addition of 35% (v/v) of Denaturing Solvents: CW EPR Results. Increasing the concentration of ethanol or Emimdca to 35% (v/v) results in a complete loss of the spectral component representing the slowly tumbling spin labels (bound FAs). At the same time, sharp three-line signals, the signature of free FAs, are

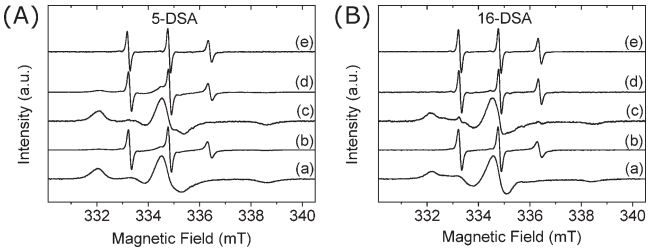

Figure 3. CW EPR spectra of 5-DSA (A) and 16-DSA (B) in HSA/buffer/15% (v/v) glycerol (a) at a FA/HSA ratio of 2 upon addition of 35% (v/v) ethanol (b), Emimdmp (c), or Emimdca (d) at room temperature. For comparison, reference spectra of 5-DSA and 16-DSA in buffer/15% (v/v) glycerol/35% (v/v) Emimdca are displayed in (e).

observed. Figure 3 shows the binding of 5- and 16-DSA to HSA at RT in buffer/glycerol solution (a) and upon addition of 35% (v/v) of ethanol (b), Emimdmp (c), or Emimdca (d). For comparison, reference spectra of 5- and 16-DSA in buffer/glycerol/35% (v/v) Emimdca solutions without HSA are displayed in Figure 3 (e).

Line shape analysis and the ΔB values found in these reference spectra without HSA are almost identical to those obtained from Figure 3(b) and (d) for both 5- and 16-DSA. Therefore, one can infer that the ensemble of all HSA molecules in the presence of 35% (v/v) of Emimdca or ethanol unfolds to a large degree and sets free almost all bound FAs. On the other hand, 35% (v/v) Emimdmp mostly preserves the bound FA signals (spectra c) in Figure 3. The phosphate-based anion has a stronger kosmotropicity than the other anions used in this study. In addition, the Emim cation is a weak kosmotropic cation. It has been shown that kosmotropic anions and chaotropic (i.e., nonkosmotropic) cations stabilize protein structures by promoting the water structure around them.[33,34] Therefore, Emimdmp addition may not distort the tertiary structure of HSA strongly, as we have already previously found for the IL choline dhp.[16]

At RT, 35% (v/v) of cosolvent yields different bound/free EPR signal ratios for 5- and 16-DSA. Ethanol or Emimdca addition yields only free 16-DSA signals, but ca. 15% of all bound 5-DSA is preserved. This could be indicative of the inner part of the denatured protein (probed by 5-DSA) being still more structured than the protein surface (probed by 16-DSA). Furthermore, in 35% (v/v) Emimdmp only a small fraction of free 16-DSA is found, while there is no free 5-DSA signal observed in this solvent mixture.

Temperature Dependence of HSA Structure: CW EPR Results. The effect of temperature on the structure of the native and unfolded states of HSA can now be examined by temperature-dependent CW EPR measurements in the range of 103−323 K. The full sets of CW EPR spectra of 5-DSA and 16-DSA in different HSA solutions (in HSA buffer/glycerol, + 35% (v/v) ethanol, + 35% (v/v) Emimdmp, + 35% (v/v) Emimdca) are displayed in the Supporting Information (Figures 3 and 4).

Figure 4 displays the comparison of 5-DSA in HSA buffer/glycerol, in 35% (v/v) Emimdca-containing solution, and in a reference solution without HSA at 230, 258, 273, and 323 K. At 230 K, all the samples show a similar nitroxide powder spectrum; i.e., the FA rotational motion is slowed down and static on the EPR time scale. At 323 K, the CW EPR spectra of 5-DSA in HSA buffer/glycerol prove that the FAs are still bound to HSA. On the contrary, the CW EPR signature of FAs in the Emimdca-containing HSA solutions at 323 K is virtually identical to that of free FAs in the reference spectra (Figure 4(B) and (C)). This is clearly indicative of the loss of binding pockets and tertiary structure of HSA that has already been presented in Figure 3. However, the temperature range in between 230 and 323 K yields unexpected CW EPR spectra for the case of FAs in Emimdca-including HSA solutions. Interestingly, between 258 and 273 K, these Emimdca-containing solutions display bimodal CW EPR spectra with signals stemming from bound and from free FAs simultaneously. This is observed neither in the normal buffered HSA solution nor in the Emimdca-based reference sample without HSA. In these samples, only one type of signal could be detected at any given temperature: bound FAs (HSA/buffer/glycerol) or free FAs (Emimdca/buffer/glycerol). These bimodal spectra of 5-DSA in Emimdca-containing HSA solutions could be explained by the existence of a certain fraction of HSA molecules being (re)folded into the native (or one close to the native) state or by all HSA being partially refolded. Note that a similar appearance of bimodal spectra and refolding of HSA were also (and only) observed in samples containing 35% (v/v) ethanol (see Supporting Information, Figures 3 and 4). Note that the same type of bimodal spectra was observed for 16-DSA in HSA samples containing 35% (v/v) ethanol or Emimdca (see Supporting Information, Figures 3 and 4), which further substantiates the conclusion that the FA binding pockets are reformed and that the protein at least partially refolds.

To obtain a detailed picture of these (re)folded structures, we used DEER spectroscopy to characterize the distribution of FAs in these samples.

Distribution of 5- and 16-DSA in HSA in the Presence of Denaturing Cosolvents. DEER spectroscopy can provide quantitative information about the conformational changes of HSA that are induced by the addition of cosolvents and may also illustrate potential refolding of HSA at low temperatures. DEER experiments are carried out on shock-frozen, vitrified protein solutions at 50 K. Note that when the samples are shock frozen a

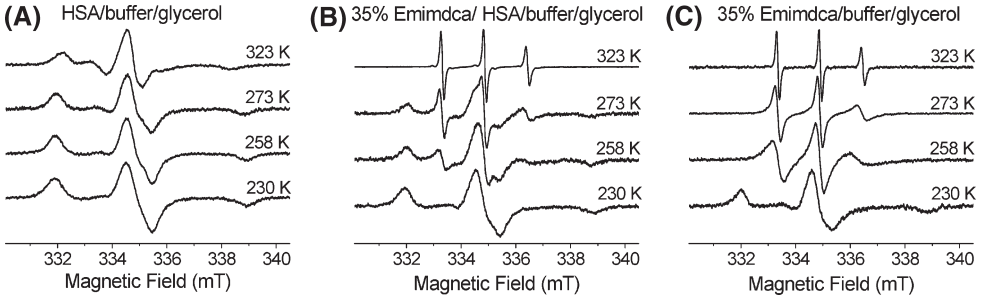

Figure 4. Temperature dependence of CW EPR spectra of 5-DSA in HSA buffer/glycerol solution (A), in 35% (v/v) Emimdca-containing HSA buffer/glycerol solution (B), and in 35% (v/v) Emimdca/buffer/glycerol/without HSA (C) at different temperatures: 230, 258, 273, and 323 K.

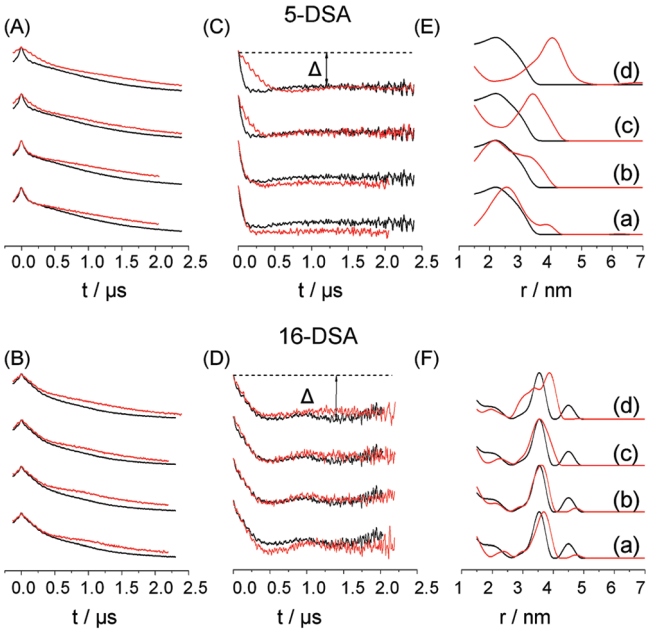

Figure 5. (A, B) Time domain DEER data, (C, D) intramolecular part of the time domain DEER data, and (E, F) distance distributions obtained by Tikhonov regularization of the 5-DSA (top; A, C, E) and 16-DSA (bottom; B, D, F) in HSA buffer/15% (v/v) glycerol (black) and upon addition of 5% (v/v) cosolvents (red) (a) ethanol, (b) Emimdmp, (c) $EmimBF_4$, or (d) Emimdca. On average, each protein is loaded with two spin-labeled FAs. The modulation depths $\Delta = 0.25$ for 5-DSA and $\Delta = 0.31$ remain almost identical regardless of solvent composition and are marked for 16-DSA.

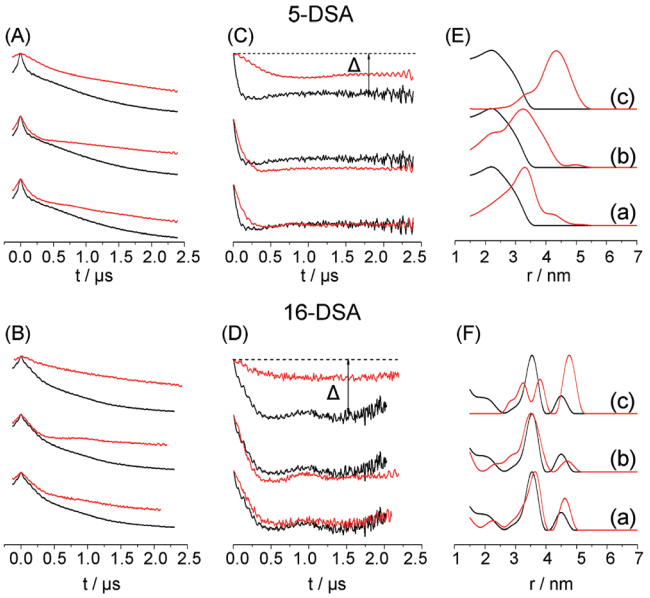

Figure 6. (A, B) Time domain DEER data, (C, D) intramolecular part of the time domain DEER data, and (E, F) distance distributions obtained by Tikhonov regularization of the 5-DSA (top; A, C, E) and 16-DSA (bottom; B, D, E) in HSA buffer/15% (v/v) glycerol (black) and upon addition of 35% (v/v) cosolvents (red) (a) ethanol, (b) Emimdmp, and (c) Emimdca. On average, each protein is loaded with two spin-labeled fatty acid molecules. The modulation depth $\Delta = 0.25$ is marked for 5-DSA, and $\Delta = 0.31$ is marked for 16-DSA.

"snapshot" of all protein conformations and molecular distributions in the sample is frozen at the glass transition temperature, when all large-scale motion ceases. We have previously conducted CW EPR and DEER measurements of aqueous ethanol-, $BmimBF_4$-, or choline dhp-containing HSA samples prepared without glycerol at 298 and 50 K, respectively.[16] The DEER signals of spin-labeled FAs in the vitrified ethanol- and $BmimBF_4$-based HSA solutions without glycerol were very weak with a poor signal-to-noise ratio. However, for the choline dhp-containing HSA sample (prepared also without glycerol), the time domain signals were similar to those in HSA buffer/glycerol solutions, and the FA distance distribution in choline dhp-based HSA was in even better agreement with the crystallographic data. Therefore, we concluded that choline dhp stabilized a specific HSA conformation close to the crystal structure. In particular, to reach much lower glass transition temperatures, we here added the 15% (v/v) of glycerol into all HSA solutions to understand the solvent and low temperature effects on the structure of HSA.

5% (v/v) Denaturing Cosolvents. The DEER data of spin-labeled FAs in a frozen solution of HSA, buffer/glycerol in the presence and absence of 5% (v/v) ethanol, Emimdmp, $EmimBF_4$, or Emimdca are displayed in Figure 5. Similarly to what could be deduced from the CW EPR results in Figure 2, 5-DSA distributions (upper part of Figure 5) in ternary mixtures in general show a stronger deviation from the native "reference" case of FAs + HSA in buffer/glycerol than the analogous 16-DSA distributions. Remarkably, DEER data of all samples containing 16-DSA are very similar, but slight yet significant deviations of the time domain signals of 5-DSA are obtained upon addition of 5% (v/v) Emimdca or $EmimBF_4$. As can be seen in Figure 5(C), the modulation depths Δ of 5-DSA are similar in the presence and absence of 5% (v/v) cosolvents, but the decay of the DEER time domain signals is slower when Emimdca or $EmimBF_4$ is added. This means that the average number of coupled spins with and without IL cosolvent remains largely identical, but the dominant dipolar coupling frequencies become lower, indicating the prevalence of longer distances between 5-DSA upon addition of $EmimBF_4$ or Emimdca (Figure 5(E)).

The corresponding DEER distance distributions (Figure 5(E) and (F)) show that Emimdca, compared to other cosolvents, causes a major change of the distance distribution of both 5-DSA and 16-DSA. A broad distance distribution of 5-DSA with a maximum around 2.2 nm increases to 4 nm, and the rather narrow distance distribution of 16-DSA with a sharp dominating distance at 3.6 nm broadens and increases to 3.8 nm upon addition of Emimdca. Adding 5% (v/v) of $EmimBF_4$ significantly increases the mean distance distribution of 5-DSA to 3.4 nm. Also, other ILs with different anions $EmimNO_3$, $EmimSO_4$, and EmimSCN yield similar DEER results as $EmimBF_4$-containing samples (Supporting Information, Figure 5). In contrast, for a sample containing 5% (v/v) ethanol or Emimdmp, the distance distributions of 5- and 16-DSA are very similar to those in buffered solutions.

The combined CW EPR and DEER results of 5- and 16-DSA suggest that the addition of low volume fractions (5% (v/v)) of denaturing cosolvents does not change the average number of coupled spin-labeled FAs bound to HSA. This also means that the FA binding pockets of HSA are largely retained. However, the tertiary structure of the HSA is affected upon addition of cosolvents. Interestingly, the inner part of the protein probed by 5-DSA is distorted much more than the protein surface probed by 16-DSA. This could be due to the already larger

flexibility of the protein at its surface as probed by 16-DSA, which may be flexible enough to adapt to the now contained third type of solvent. The shift in average distance detected for 5-DSA in particular when BF_4^- or dca^- are used as anions could be due to two reasons. First, one may imagine that these two anions can occupy FA binding pockets in competition with our spin-labeled FAs and may block certain binding sites for the FAs. The second explanation could be that these two ILs can enter the protein and may lead to a change in distribution of the FA anchor points due to specific IL cation or anion interactions with certain amino acids in the protein. The first explanation seems rather unlikely, as it would imply that the IL anions have such a high binding affinity at only certain binding sites that they can fully prevent FA binding. Nonetheless, with our data at hand we cannot finally settle this question at this point.

35% (v/v) Denaturing Cosolvents. Similar to the CW EPR results for Emimdca, in 35% (v/v) ethanol-containing samples at 298 K, mainly free 5-DSA signals are found, while at lower temperature (273 K, see Supporting Information Figure 3) also bimodal (free and bound) 5-DSA signals are observed. DEER measurements on ethanol-containing samples at 50 K feature a modulation depth (Δ = 0.25) similar to that in the sample without ethanol (Figure 6). This surprising finding can only be explained when FAs that are not bound to HSA at RT bind to refolded albumin at low temperatures, as we already deduced earlier from the CW EPR results. However, the decay of the DEER signal is slower in the case of the ethanol-containing sample, which reflects the longer distances between 5-DSA as compared with the case in buffered sample. The broad distance distribution of 5-DSA with a maximum around 2.2 nm increases to 3.3 nm with 35% (v/v) ethanol (Figure 6).

For the sample with 35% (v/v) Emimdca, the modulation depth and the average number of coupled spins of 5-DSA (Δ = 0.13, N = 1.5) are smaller than those in buffered sample (Δ = 0.25, N = 2.0). The decrease in modulation depth is evidence of the displacement of a significant fraction of FAs from the protein. Although the average number of coupled FAs decreases (and only those cases contribute where two FAs are bound simultaneously to one HSA), 1.5 is still a significant number in particular considering that CW EPR spectra show that almost all FAs are free (unbound) at RT. This supports our findings from low-temperature CW EPR, where a significant fraction of FAs were observed that exhibit the spectral signature of FAs bound to HSA. Therefore, one can infer that unfolded HSA upon addition of Emimdca is partially refolded at the glass transition temperature. In addition, to exclude that the measured dipolar couplings and distance distributions are due to some kind of micelle formation of FAs in the ternary solvent mixture, we have performed control DEER experiment of FAs using 35% (v/v) of Emimdca in buffer/glycerol solution but without HSA. In this solution, only mobile FAs are seen in CW EPR (see Figure 4), and with DEER no dipolar coupling between spin-labeled FAs can be detected (Supporting Information, Figure 6).

The distance distribution of bound 5-DSA in the 35% (v/v) Emimdca-containing sample deviates strongly from that in the buffered sample. In this case, the broad distance distribution with a maximum around 2.2 nm increases to 4.3 nm. This finding suggests that a stronger structural change of HSA takes place when Emimdca is added as compared to the case of ethanol addition (see Figure 6). This could, e.g., be due to partial refolding, where some secondary structure elements reassemble into their native tertiary structure and form binding pockets but some others do not.

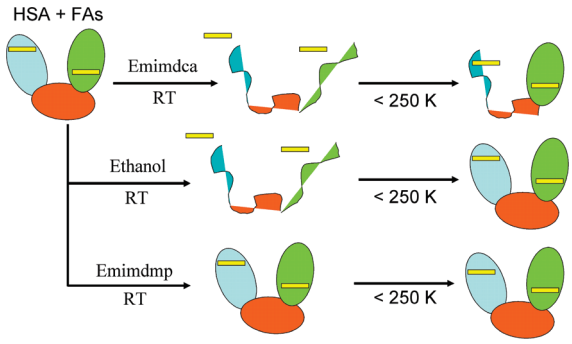

Figure 7. Schematic representation of the proposed solvent-induced refolding of denatured HSA at low temperatures. Two FAs are bound to HSA at the native state. At RT, addition of Emimdca or ethanol unfolds HSA and sets free almost all bound FAs, but addition of Emimdmp preserves bound FAs. Denatured HSA upon addition of ethanol or Emimdca refolds at low temperatures (<250 K).

As could be expected from the CW EPR results at RT, the sample with 35% (v/v) Emimdmp gives a DEER signal for 5-DSA that is similar to that in buffered solutions. The modulation depth in the Emimdmp-containing sample (Δ = 0.30, N = 2.2) is slightly larger than that of buffered sample for 5-DSA (Δ = 0.25, N = 2.0) with a slower decay of the DEER signal. The maximum in the distance distribution thus increases to 3.3 nm.

The DEER results for 16-DSA are displayed in Figure 6, too. The modulation depth of the 35% (v/v) Emimdca-containing sample (Δ = 0.10) is much lower than the modulation depth in the respective buffered sample (Δ = 0.31). Thus, the average number of coupled 16-DSA spins in the protein decreases upon addition of Emimdca from N = 2.0 to N = 1.3. In addition, the distance distribution of 16-DSA changes considerably. The characteristic distance peak of 16-DSA in native HSA at 3.6 nm weakens, and a sharp dominating signal at 4.8 nm appears upon addition of Emimdca.

Although 35% (v/v) Emimdmp or ethanol addition increases the distances between bound 5-DSA, the main distance peak for bound 16-DSA is preserved. This could suggest that the inner, more rigid part of the protein probed by 5-DSA is much more strongly affected upon addition of 35% (v/v) of ethanol or Emimdmp. This, of course, is seemingly counterintuitive, as one would expect that solvent-induced changes in protein conformation proceed from the surface to the interior. One should note that the surface of the protein as probed by 16-DSA has a large conformational flexibility and presents a highly symmetric distribution of binding pocket entrances in its native state. In this case, this large flexibility may have the effect that HSA could be more tolerant against denaturation on the surface: while interaction of the charged amino acids in the interior with ethanol or $Emim^+$ and dmp^- ions may lead to a "widening" or rearrangement in the interior, the overall protein surface presented may still largely resemble that of the native state.

Finally, the results of the CW EPR and DEER applied to HSA solutions in the presence of denaturants suggest that the concentration of cosolvents determines the degree of protein unfolding and refolding at high and low temperatures, respectively. Addition of 42% (v/v) ethanol or Emimdca (the highest volume fraction that yields homogeneous mixtures at RT) to the protein solution yields a much lower DEER modulation depth

with longer distances between fewer coupled FAs (Supporting Information Figure 7). Therefore, the presence of a denaturant solvent with a higher concentration not only increases HSA unfolding at RT but also decreases its refolding at low temperatures.

Our CW EPR and DEER-derived findings are combined in the schematic representation of the proposed solvent-induced denaturation at RT and refolding of HSA at low temperatures (Figure 7). It is long-established knowledge that ethanol serves as a denaturing solvent at RT. Here we show that the decrease of temperature of ethanol-containing HSA samples causes almost complete protein refolding in the presence of glycerol. Furthermore, even unfolded HSA upon addition of Emimdca—which is a stronger denaturing solvent than ethanol—partially refolds again at low temperatures in the presence of glycerol (but on average only 1.5, not 2, FAs are bound again). Thus, at the lower temperatures one can infer that interaction between the denaturants and the protein may become weaker. The reason for this could be the cryoprotective and stabilizing effects of glycerol, which had already been described for other proteins before.[13] With temperature also the preferential solvation around the protein changes, and in ternary mixtures as used in this study, glycerol may well preferentially solvate HSA (in particular the surface) and replace the denaturing solvents that strongly solvate and influence the protein at higher temperature (RT and above). Together with the increased HSA stability and propensity to refold at lower temperatures, this may lead to the observed partial (Emimdca) and almost full refolding (ethanol) of the protein.

Our results are representative for one system of protein and ligands, namely, HSA and long-chain FAs. HSA is a model protein that combines well-folded structures and conformational flexibility in solution, and yet, it appears plausible that analogous effects may be found for other proteins in similar ternary solvent mixtures if low temperatures can be reached before complete freezing of the systems.

CONCLUSION

At RT, the CW EPR data of spin-labeled FAs (5- and 16-DSA) in HSA buffer/glycerol solutions show that a high concentration of cosolvents (ethanol or Emim-based ILs) denature the protein. The addition of the 35% (v/v) of ethanol or Emimdca results in a loss of the EPR spectral contribution of bound FAs and yields only the signal of unbound FAs, which can be clearly separated due to their strongly different rotational dynamics. However, at lower temperatures (approx. 250−280 K), the signal of bound FAs reappears simultaneously with that of unbound FAs. This bimodal spectrum is only observed for the admixture of denaturing cosolvents to the aqueous/glycerol protein solutions and not observed for the samples without HSA or in binary solvent mixtures. This suggests that FAs are at least partially bound to the protein again at lower temperatures.

DEER measurements substantiate the CW EPR results and shed light on the protein-structural changes that take place. The DEER data of spin-labeled FAs in 35% (v/v) ethanol-containing HSA buffer/glycerol solution are very similar to those of HSA buffer/glycerol solutions, where HSA is in the native state. The average numbers of dipolar-coupled spins (i.e., FAs bound to HSA) are the same for both samples, which suggests almost complete refolding of the denatured protein at the glass transition temperature. The distance distribution of 16-DSA in HSA solution in the presence of ethanol is also very similar to that of the native state. In contrast, the distance distribution of 5-DSA shifts to higher values upon addition of ethanol. This suggests that the more rigid inner part of the protein probed by 5-DSA features a slightly different structure upon addition of ethanol at 50 K, but the surface of the protein probed by 16-DSA is comparable with the surface of the native HSA structure. Since the inner part of the protein is very rigid compared to the surface of the protein, a little structural variation causes a larger distance distribution deviation in the case of 5-DSA.

The denaturation of HSA upon addition of ILs depends on the chaotropic properties of anions. Emimdca is the strongest denaturing solvent for HSA at RT in this study. The free FAs in 35% (v/v) Emimdca-containing HSA buffer/glycerol solution are bound to HSA again at lower temperatures than in the 35% (v/v) ethanol-containing sample. This is explained by the reduced stability of HSA in the Emimdca-containing sample. Also, DEER reveals a lower average number of bound FAs in the Emimdca-including sample compared to that in other HSA solutions, and the distance distribution of FAs is also much more affected after the Emimdca addition. Despite the strong denaturation effect of Emimdca on the HSA at RT, the protein structure seems to at least partially refold at lower temperatures.

The refolding in ternary solvent mixtures may be a general effect found for certain proteins in such ternary solvent mixtures and may basically be traced back to the preferential solvation of HSA by glycerol at lower temperatures and the increased stability of the protein's tertiary structure at the lower temperatures that can be reached in such solvent systems.

ASSOCIATED CONTENT

Supporting Information. Experimental and simulated CW EPR spectra of 5-DSA and 16-DSA in HSA/buffer/15% (v/v) glycerol upon addition of 5% (v/v) of cosolvents. EPR parameters from simulation of CW spectra of 5-DSA and 16-DSA bound to HSA. CW EPR spectra of 5-DSA in HSA/buffer/15% (v/v) glycerol upon addition of 5% (v/v) of cosolvents. Time domain DEER data, intramolecular part of the time domain DEER data, and distance distributions obtained by Tikhonov regularization of the 5-DSA in HSA buffer/15% (v/v) glycerol and upon addition of 5% and 42% (v/v) cosolvents. Temperature dependency of CW EPR spectra of 5-DSA and 16-DSA in HSA buffer/glycerol, in 35% (v/v) ethanol-including HSA buffer/glycerol, in 35% (v/v) Emimdmp-including HSA buffer/glycerol, in 35% (v/v) Emimdca-including HSA buffer/glycerol, and in 35% (v/v) Emimdca/buffer/glycerol/without HSA at different temperatures between 103 and 323 K. This material is available free of charge via the Internet at http://pubs.acs.org.

AUTHOR INFORMATION

Corresponding Author

*E-mail: dariush.hinderberger@mpip-mainz.mpg.de. Tel.: +49 6131 379 126. Fax: +49 6131 379 100.

ACKNOWLEDGMENT

We thank Prof. Dr. Hans W. Spiess for helpful discussions and Christian Bauer for technical support. This work was financially supported by the Deutsche Forschungsgemeinschaft (DFG)

under grant number HI 1094/2-1 (DH) and by the Max Planck Graduate Center with the University of Mainz (MPGC (DH)).

REFERENCES

(1) Tanford, C. *Adv. Protein Chem.* **1968**, *23*, 121–282.
(2) Peters, T. *All About Albumin: Biochemistry, Genetics and Medical Applications*; Academic Press: San Diego, 1995.
(3) Tilton., R. F.; Dewan, J. C.; Petsko, G. A. *Biochemistry* **1992**, *31*, 2469–2481.
(4) Whitten, S. T.; Kurtz, A. J.; Pometun, M. S.; Wand, A. J.; Hilser, V, J. *Biochemistry* **2006**, *45*, 10163–10174.
(5) Pastore, A.; Martin, S. R.; Politou, A.; Kondapalli, K. C.; Stemmler, T.; Temussi, P. A. *J. Am. Chem. Soc.* **2007**, *129*, 5374–5375.
(6) Flora, K.; Brennan, J. D.; Baker, G. A.; Doody, M. A.; Bright, F. V. *Biophys. J.* **1998**, *75*, 1084–1096.
(7) Michnik, A.; Drzazga, Z. *J. Therm. Anal. Calorim.* **2007**, *88*, 449–454.
(8) Privalov, P. L. *Crit. Rev. Biochem. Mol. Biol.* **1990**, *25*, 281–305.
(9) Griko, Y. U.; Privalov, P. L.; Sturtevant, J. M.; Venyaminov, S. Y. *Proc. Natl. Acad. Sci. U.S.A.* **1998**, *85*, 3343–3347.
(10) Kitahara, R.; Okuno, A.; Kato, M.; Taniuchi, Y.; Yokoyama, S.; Akasaka, K. *Magn. Reson. Chem.* **2006**, *44*, S108–S113.
(11) Taborsky, G. *Adv. Chem.* **1979**, *180*, 1–26.
(12) Sousa, R. *Acta Cryst. D* **1995**, *51*, 271–277.
(13) Rariy, R. V.; Klibanov, A. M. *Proc. Natl. Acad. Sci. U.S.A.* **1997**, *94*, 13520–13523.
(14) Page, T. A.; Kraut, N. D.; Page, P. M.; Baker, G. A.; Bright, F. V. *J. Phys. Chem. B* **2009**, *113*, 12825–12830.
(15) Baker, G. A.; Heller, W. T. *Chem. Eng. J* **2009**, *147*, 6–12.
(16) Akdogan, Y.; Junk, M. J. N.; Hinderberger, D. *Biomacromolecules* **2011**, *12*, 1072–1079.
(17) Wasserscheid, P.; Keim, W. *Angew. Chem., Int. Ed.* **2000**, *39*, 3772–3789.
(18) Pàrvulescu, V. I.; Hardacre, C. *Chem. Rev.* **2007**, *107*, 2615–2665.
(19) Chen, X.; Liu, J.; Wang, J. *Anal. Methods* **2010**, *2*, 1222–1226.
(20) Hubbell, W. L.; Cafiso, D. S.; Altenbach, C. *Nat. Struct. Biol.* **2000**, *7*, 735–739.
(21) Steinhoff, H.-J. *Biol. Chem.* **2004**, *385*, 913–920.
(22) Jeschke, G.; Polyhach, Y. *Phys. Chem. Chem. Phys.* **2007**, *9*, 1895–1910.
(23) Bhattacharya, A. A.; Grüne, T.; Curry, S. *J. Mol. Biol.* **2000**, *303*, 721–732.
(24) Hamilton, J. A.; Cistola, D. P.; Morrisett, J. D.; Sparrow, J. T.; Small, D. M. *Proc. Natl. Acad. Sci. U.S.A.* **1984**, *81*, 3718–3722.
(25) Junk, M. J. N.; Spiess, H. W.; Hinderberger, D. *Angew. Chem., Int. Ed.* **2010**, *49*, 8755–8759.
(26) Junk, M. J. N.; Spiess, H. W.; Hinderberger, D. *J. Magn. Reson.* **2011**, *210*, 210–217.
(27) Junk, M. J. N.; Spiess, H. W.; Hinderberger, D. *Biophys. J.* **2011**, *100*, 2293–2301.
(28) Pannier, M.; Veit, S.; Godt, A.; Jeschke, G.; Spiess, H. W. *J. Magn. Reson.* **2000**, *142*, 331–330.
(29) Jeschke, G.; Pannier, M.; Spiess, H. W. In *Biological Magnetic Resonance: Distance Measurments in Biological System by EPR*; Kluwer Academics: New York, 2000; Vol. 19.
(30) Jeschke, G.; Bender, A.; Paulsen, H.; Zimmermann, H.; Godt, A. *J. Magn. Reson.* **2004**, *169*, 1–12.
(31) Jeschke, G.; Chechik, V.; Ionita, P.; Godt, A.; Zimmermann, H.; Banham, J.; Timmel, C. R.; Hilger, D.; Jung, H. *Appl. Magn. Reson.* **2006**, *30*, 473–498.
(32) Bode, B. E.; Margraf, D.; Planckmeyer, J.; Dürner, G.; Prisner, T. F.; Schiemann, O. *J. Am. Chem. Soc.* **2007**, *129*, 6736–6745.
(33) Fujita, K.; MacFarlane, D. R.; Forsyth, M.; Yoshizawa-Fujita, M.; Murata, K.; Nakamura, N.; Ohno, H. *Biomacromolecules* **2007**, *8*, 2080–2086.
(34) Constantinescu, D.; Herrmann, C.; Weingärtner, H. *Phys. Chem. Chem. Phys.* **2010**, *12*, 1756–1763.